# Admittometric Electrochemical Determination of Atrazine by Nano-composite immune-biosensor using FFT- Square wave Voltammetry

P. Norouzi[1,2,*], B. Larijani,[2,*] M. R. Ganjali[1,2], F. Faridbod[1,2]

[1]Center of Excellence in Electrochemistry, University of Tehran, Tehran, Iran
[2]Endocrinology & Metabolism Research Center, Tehran University of Medical Sciences, Tehran, Iran
*E-mail: norouzi@khayam.ut.ac.ir

A novel atrazine electrochemical measurement system was developed based on antibody combine with Au nanoparticles, Multi walled carbon nanotube and ionic liquid on glassy carbon electrode surface. Coulometric fast Fourier transformation square wave voltammetry was used for the electrochemical measurements. In this method, the admittance response of the electrode was integrated in a selected potential range to calculate amount of transferred charge during the adsorption of atrazine. Analytical parameters such as pH, SW frequency, amplitude and deposition time of Au were also studied. The linear concentrations range of atrazine was from 0.5–100 nM with a detection limit of 0.02 nM. Moreover, the proposed sensor exhibited good accuracy, low response time, which was less than 9 s, high sensitivity with repeatability (R.S.D value of 3.7%) and long term stability, 40 days with a decrease of 8.9% in response.

## 1. INTRODUCTION

Pesticides and herbicides are widely used in agriculture, and hence cause heavy environmental pollutions. Especially it is a serious problem in surface and ground waters. Atrazine (2-chloro-4-ethylamino-6-isopropylamino-s-triazine) (Fig. 1) is one of the most popular herbicides among the triazine group and efficiently employed for control of grassy and broadleaf weeds in sorghum, maize, sugarcane, and other crops as well as in non-cropland situations [1].

Atrazine shows phytotoxic effects, which include inhibition photolysis and photosynthesis, decomposition of chloroplast, diminishing the carbohydrate content, suppression of tissue respiration,

and changes in the enzyme activity [2]. It may be also dangerous for human health because it is suspected to cause cancers, birth defects and interruption of hormone functions [3]. Therefore, the development of sensitive, cheap, simple, and rapid analytical methods is very crucial for monitoring the presence and amounts of pesticides and preventing toxicological risks.

Some techniques have been reported for determination of atrazine, such as high-performance liquid chromatography (HPLC) [4], gas chromatography (GC) [5], liquid chromatography–mass spectrometry (LC–MS) [6], gas chromatography–mass spectrometry (GC–MS) [7], thin-layer chromatography (TLC) [8], potentiometery [9], spectrophotometric method [10] and enzyme immunoassay [11].
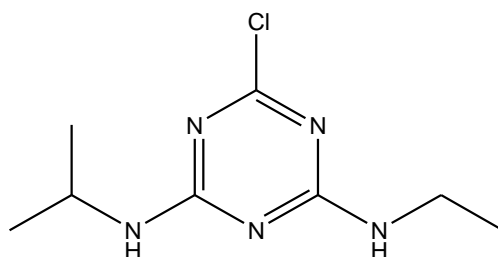


**Figure 1.** Chemical structure of Atrazine

Electrochemical Impedance Spectroscopy (EIS) is a relatively new and powerful technique to characterize the electrical properties of materials [12], surface-modified electrodes [13,14] for study the electrochemical processes [15]. It is used in study of dynamics of bound or mobile charge in the bulk or interfacial regions of any kind of material (solid or liquid) [15]. Electrochemical impedance spectroscopy (EIS) is a sensitive technique based on monitoring the electrical response of a device after application of a periodic small amplitude AC signal in a wide range of frequencies (typically, from 100 kHz to 0.1 Hz, for biosensors). The analysis of the impedance values measured provides information concerning the electric properties of the sensor–sample interface and the underlying reactions [16,17]. Impedance spectroscopy offer important advantages for the development of diagnostic devices. It requires the application of only a small perturbation (usually sinusoidal) [14,15], which reduces the matrix interferences in analytical systems, involves relatively simple electrical measurements, can readily be automated, the results may often be correlated with many complex material variables and it can predict aspects of the performance of chemical sensors and fuel cells [12].

In this work, a new electrochemical method based on modern voltammetry and an immunosensor was developed. The proposed immunosensor is characterized by electrochemical EIS and Fast Fourier Transformation (FFT) voltammetry. The approach used here is designed to separate the voltammetric signal and background signal in frequency domain by using discrete FFT method [18-35]. This separation allows, digitally filtrating some of the noises and decreasing the bandwidth of the measurement. Further improvement in the signal was obtained by two-dimensional integration of the electrode response over a selected potential range and time window of the signal. Using multi-

walled carbon nanotubes (MWCNT) and ionic liquids on the electrode surface improves the conductivity of the sensor, and increases the transduction of the chemical signal to electrical signal.

## 2. MATERIALS AND METHODS

### 2.1. Reagents

Atrazine, potassium ferricyanide, sodium chloride, potassium chloride, sodium phosphate dibasic ($Na_2HPO_4$), sulfuric acid (98%), ethanol (98%), poly(ethylene glycol 400 diglycidyl ether) (PEGDGE), and 1-butyl-3-methylimidazolium tetrafluoroborate (BMIM-$BF_4$, ionic liquid, IL) were of analytical grades and purchased from Merck. The MWCNT was purchased from Research Institute of the Petroleum Industry (Iran).The buffer solution used for the experiments was phosphate buffered (PBS), 3 mM KCl, 0.1 mM $Na_2HPO_4$, 1.8 mM $KH_2PO_4$, pH 7.0. The redox couple $Fe(CN)_6^{3-}/Fe(CN)_6^{4-}$ at a 5 mM concentration was also prepared. The solutions were kept at 4 °C before use. The polyclonal anti-atrazine antibody was purchased from Chemicon Company. Bovine serum albumin (BSA) was from Sigma.

### 2.2. The sensor preparation

A glassy carbon electrode (GCE, 3 mm in diameter) was polished with 1.0, 0.3 and 0.05 μm alumina slurry. Then it was washed thoroughly with doubly distilled water. The electrodes were successively sonicated in 1:1 nitric acid, acetone and doubly distilled water, and then allowed to dry at room temperature. For construction of IL-MWCNTs/GCE, MWCNTs suspension in ionic liquid (2-25 μL) was dropped onto the surface of the GCE.
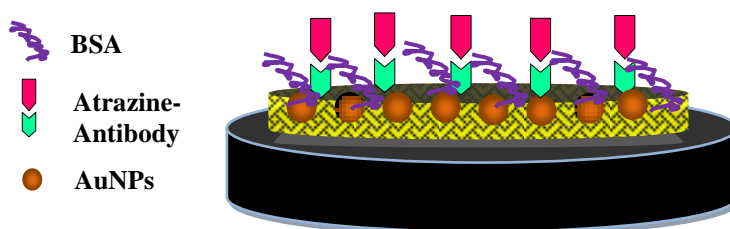


**Figure 2.** Schematic figures of the sensor preparation

Gold nanoparticles were then produced by reducing $HAuCl_4$ with sodium citrate at 100 °C for half an hour. The mean size of the prepared Au colloids was about 20-60 nm, estimated by transmission electron microscopy in a separate experiment. A mixture of 0.5 μl commercial antibody

solution (2.5 g/l) and 1 µl of PEGDGE (2.5 g/l) as a cross-linker were then loaded onto the nano-modified glassy carbon electrode surface.

Functionalized electrode was immersed in $10^{-7}$ M solution of BSA in PBS at pH 7.0, for 2 h in order to block the free space between the species. The electrode was then thoroughly rinsed with PBS to remove excess of BSA. The prepared biosensor was stored at 4 °C in PBS before use. The schematic diagram of the construction of the biosensor is shown in figure 2.

## *2.3. Instrumentation and Data Acquisition and Processing*

For the electrochemical measurement, a homemade potentiostat was used, which was connected to a personal computer. Also, an analog to digital data acquisition board (PCL-818H, Advantech Co.) was used for controlling the potentiostat and data acquisition. A special electrochemical software was developed in Delphi 6.0 environment for applying the electrochemical methods and data processing. Moreover, the program was used to generate an analog waveform and acquire current readings. EIS measurements were performed in 5 mM $K_3Fe(CN)_6$ in PBS at pH 7.0. A stock solution of 5 mM ATR was firstly prepared, and then an aliquot was diluted to the appropriate concentration. Before each measurement, the three-electrode system was installed in a blank solution, and the peak current voltammetry scan.

## 3. RESULTS AND DISCUSSION

In this detection method, the admittance of the electrode in solution could be used as a valuable tool to monitor the concentration of ATR at the surface of the immunosensor, due to this fact that adsorption of the analyte molecules on the surface of immunosensor decreases total measured admittance.

To demonstrate these changes in the admittance by the analyte, at first, EIS measurement was used. Fig. 3 shows the Nyquist plots of immunosensor for ATR at concentrations 0 to 50 nM. The Randle modified equivalent circuit was used to fit the EIS data and to determine electrical parameter values for each concentration. As shown in Fig. 3 (inset), the circuit includes the electrolyte resistance between working and reference electrodes ($R_s$); Warburg impedance ($Z_w$), resulting from the diffusion of ions to the interface from the bulk of the electrolyte; electron-transfer resistance ($R_{et}$); and electrode/electrolyte interface capacitance($C$). As indicated from the data validation, carried out by the Kramers–Kronig test, proves that experimental results fit reasonably and is in a good agreement with the proposed circuit model ($x^2 \leq 10^{-5}$). In fact, the value of $Z_w$ gives information about the diffusion of $[Fe(CN)_6]^{3-/4-}$ through the surface layer of the immunosensor, while the $R_s$ values depend on the solution. In addition, $C$ models the capacitive behavior of the double layer replacing the infrequently ideal capacitance and diffusion behavior. The values of $R_{et}$ increases significantly upon adsorption ATR on the electrode surface with concentration, reflecting the more hindered charge transfer diffusion.
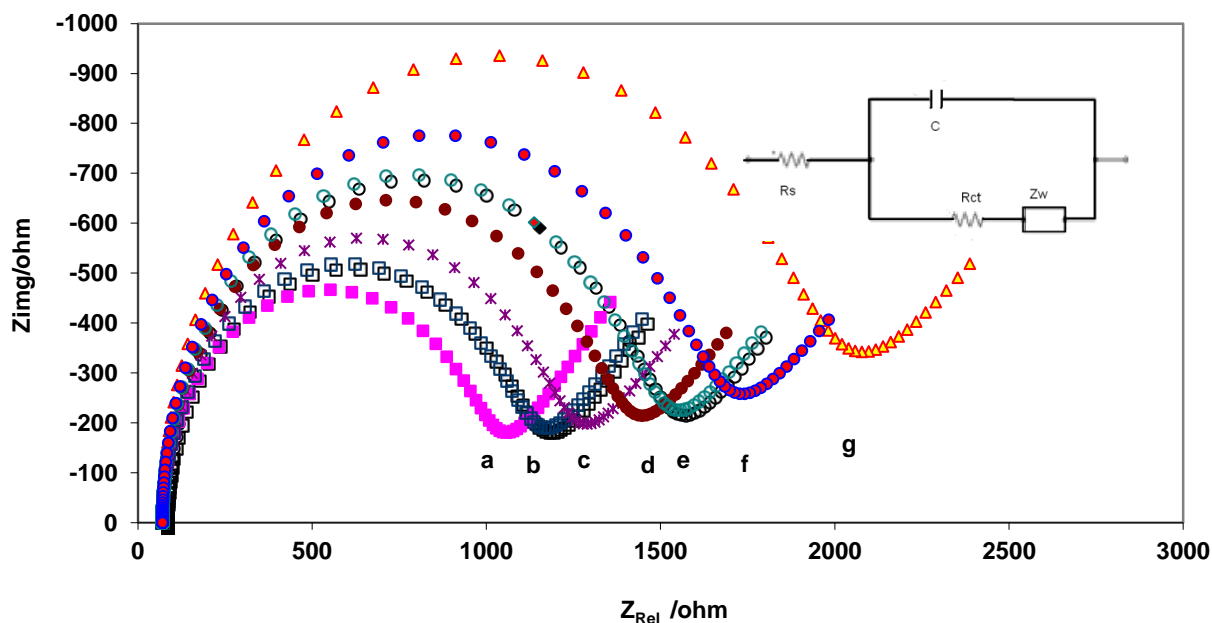
**Figure 3.** Nyquist plots of EIS spectra of  after interaction with different concentrations of ATR, in PBS at pH 7.0, 3 mM KCl, 0.1 mM $Na_2HPO_4$, 1.8 mM $KH_2PO_4$, and the redox couple $Fe(CN)_6^{3-}/Fe(CN)_6^{4-}$ 5 mM. (a) 0 nM, (b) 0.5 nM, (c) 2.0 nM, (d) 4.0 nM, (e) 10.0 nM, (f) 20.0 nM, (g) 50.0 nM of ATR.

For determination of ATR a modern electrochemical method was used to calculated admittance of the immunosensor based on FFT-SW voltammetry. In the traditional Osteryoung SWV method, the current is sampled at two points (at the end of each pulse in one SW cycle).  Whereas, in the FFT-SW voltammetry, the current s was sampled eight times each SW cycle; $t_1$ to $t_4$ (for the first SW pulse) and $t_1$ to $t_4$ (for the second SW pulse). In fact, in discrete FFT analysis, the number of sampled currents at each pulse cycle must be represented by $2n$ (where $n$ is an integer and greater than 1). Therefore the currents, $i_s$, were sampled at even time intervals, $t_s$,

$$t_s = 1 + \frac{s}{4f_0} \tag{1}$$

Where $s$ is an integer number and changes from 0 to 3. Therefore, If currents are sampled (at even time intervals, $t_s$, $t_s+1/4f_0$, $t_s+2/4f_0$ and $t_s+3/4f_0$, then the values of the sampled currents is,

$$i_k = \sum_{n=1} A_n \sin(kn\pi / 2 + 2n\pi f_0 t_s + \phi_n) \tag{2}$$

where $k$ is the number of  current data and n is the number of the potential step. To calculate the FFT-SW admittance of the immunosensor response, at first, the real and imaginary components of the alternating of current need to be calculated.

The real component of *I'* and *E'* are given by,

$$I_k = i_k - i_{k-2} \qquad (3)$$

$$E_k = E_k - E_{k-2} = -2E_s \qquad (4)$$

and the equation for the imaginary components are,

$$I'_k = i_{k-1} - i_k \qquad (5)$$

$$E_k' = E_{k-1} - E_k = 2E_s \qquad (6)$$

and the real , Y,  imagery, Y', admittance are calculated by this equation,

$$Y - jY' = \frac{I - I'}{E - E'} \qquad (7)$$

Moreover, for the calculating the immunosensor, the absolute changes in the admittance voltammogram in form of coulomb (Q) was measured based on response integration, a total absolute difference function $\Delta Q_n$ can be calculated by using the following equation:

$$\Delta Q_n = Q_n - Q_{ave} \qquad (8)$$

or

$$\Delta Q\,(s\tau) = \Delta t\left[\sum_{E=E_i}^{E=E_v}\left|A(s,E).E - A(s_r,E).E\right|\right] \qquad (9)$$

Where, *s* is the sweep number, $\tau$ is the time period between subsequent sweeps, $\Delta t$ is the time difference between two subsequent points on the admittance curves, *A(s, E)* represents the admittance of the FFT-SW voltammograms recorded during the s-th sweep and *A(s$_r$, E)* is the reference admittance of the admittance voltammograms. $E_i$ and $E_v$ are the initial and the vertex potential, respectively. The reference FFT-SW admittance curve was obtained by averaging 5 FFT-SW admittance voltammogram before addition of the ATR sample solution.  $Q_{ave}$ and $Q_n$ are the calculated average charges under the peak at the selected potential range, $E_1$ to $E_2$, from *m* FFT-SW voltammograms and the calculated charge under the peak at the same potential range from  subsequent $n^{th}$ cyclic voltammogram, respectively.

 Fig.4 shows subtracted admittance, dA, (subtracting the reference FFTAV form the other FFT-SW admittance voltammograms, dA) and the changes in the immunosensor response in the potential range of -100 to 1000 mV [14-17].  The figure shows that after addition of 10 nM ATR in the PBS buffer solution at pH 7.0. The integration range for dA is in range of 0 to 700 mV. Addition of ATR samples increases the immunosensor response (in form of $\Delta Q$, see figure 4B).
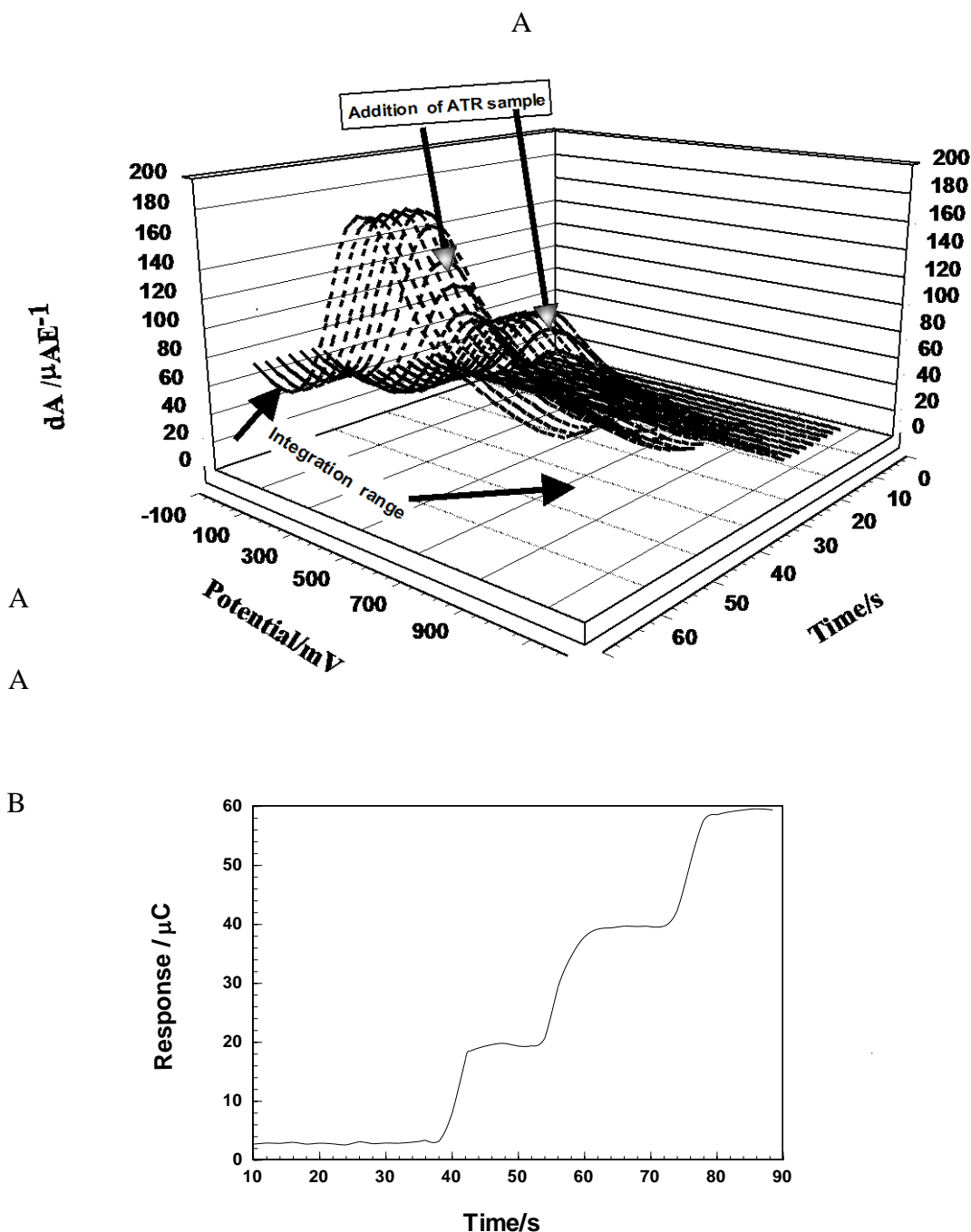
**Figure 4.** A) FFT-SW voltammograms of the immunosensor without (in absent) and with addition of 600 μL of 10 nM ATR in PBS, containing, 3 mM KCl, 0.1 mM $Na_2HPO_4$, 1.8 mM $KH_2PO_4$, pH 7.0 and the redox couple $Fe(CN)_6^{3-}/Fe(CN)_6^{4-}$ 5 mM, in the potential range of -100 to 1000 mV at frequency 500 Hz, and amplitude 20 mV and the potential integration range for the differentiated admittance. B) The calculated response of the immunosensor based on Eq.9.

The results show that with increasing the concentration of ATR in the added sample linearly increases ΔQ. In order to maximize the immunosensor response, ΔQ, the most important parameters in the detection system were optimized.

## 3.1. Effect of pH

It is well know that, the performance of the immunosensor strongly depends on the solution pH. The results of the measurements of the immunosensor response (ΔQ) in the pH range of 5.5–8.0 is shown in Fig. 5, it indicates that ΔQ response realizes to maximum at pH 7.0, where the activity of the immunosensor is the highest. Obtaining the best detector response for ATR at pH 7 may due to this fact that ATR may possibly hydrolyze in acidic and basic solution [36]. Consequently, in this measurement method, the pH of the sample solutions was adjusted near to7 for obtaining stable sample solution of ATR and immunosensor response.  Also, the changes in pH may affects on the activity of the enzyme [36].
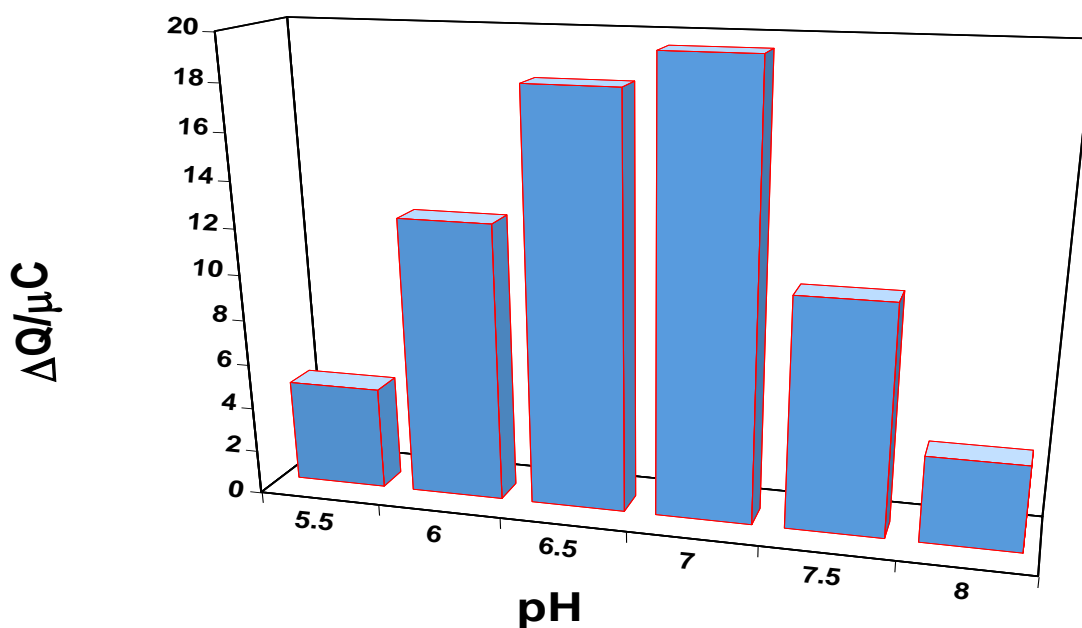


**Figure 5.** The effect of pH on the response of the immunosensor to 10 nM of ATR in PBS containing, 3 mM KCl, 0.1 mM $Na_2HPO_4$, 1.8 mM $KH_2PO_4$, pH 7.0 and the redox couple $Fe(CN)_6^{3-}/Fe(CN)_6^{4-}$  5 mM

## 3.2 Optimization of the important parameters

In the FFT-SW voltammetric measurements, the SW frequency and amplitude are important factors for the immunosensor performance and the existing background noise. In this direction, to gain the best values of frequency and amplitude for the applied SW waveform during the determination of ATR, the SW frequency range 100-1000 Hz and amplitude 2 to 40 mV were examined. In Fig. 6 the importance of frequency and amplitude is demonstrated for the solution containing of 8 nM of ATR in 3 mM KCl, 0.1 mM $Na_2HPO_4$, 1.8 mM $KH_2PO_4$, pH 7.0 and the redox couple $Fe(CN)_6^{3-}/Fe(CN)_6^{4-}$ at a 5 mM solution.

It should be noted that the solution resistance, surface of the immunosensor, and stray capacitance of the system could limit the obtained sensitivity by increasing the SW frequency. On the other hand, increasing the SW frequency and amplitude up to certain vaule can increase the the immunosensor response.
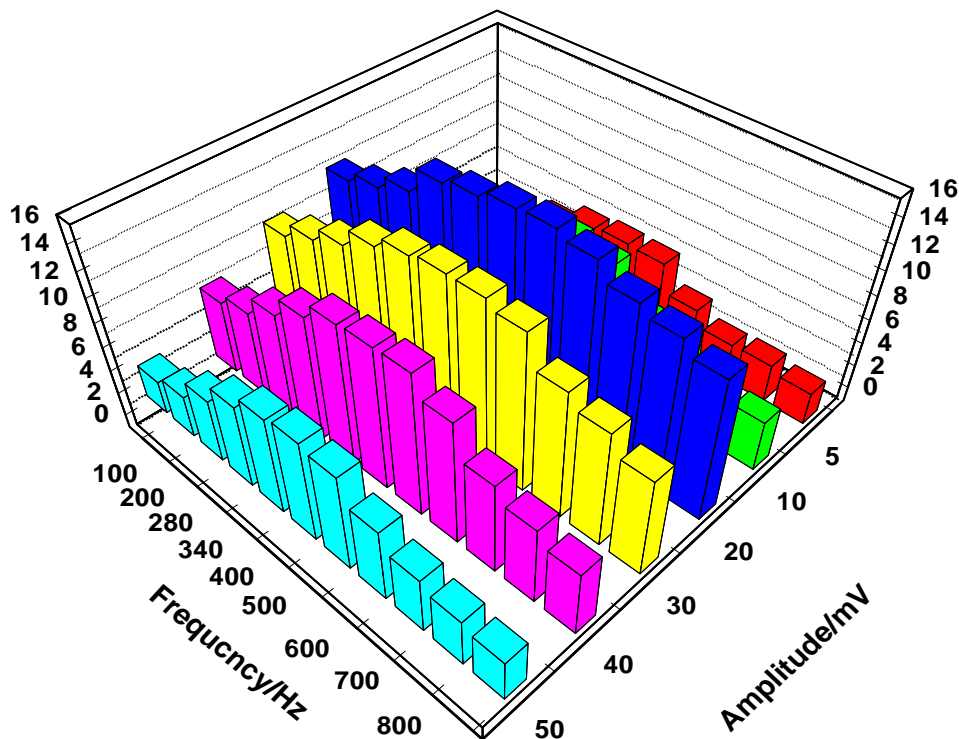


**Figure 6**. The effect of frequency and amplitude on the immunosensor in additions of 8 nM ATR and 3 mM KCl, 0.1 mM $Na_2HPO_4$, 1.8 mM $KH_2PO_4$, and the redox couple $Fe(CN)_6^{3-}/Fe(CN)_6^{4-}$ 5 mM.
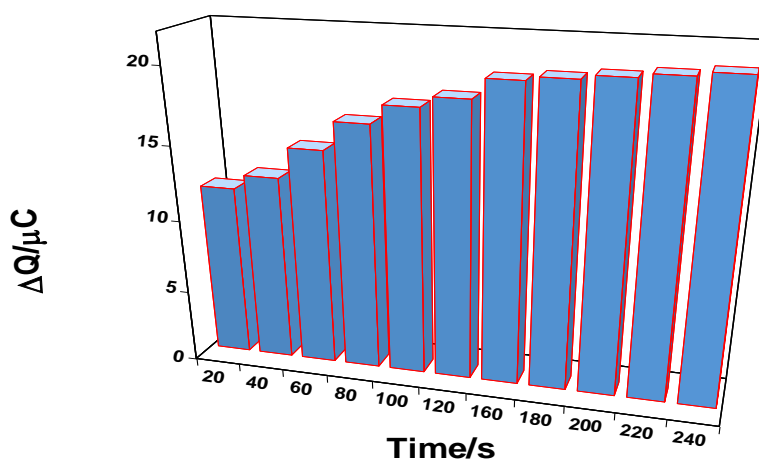


**Figure 7.** the effect of time of AuNPs deposition on the immunosensor response, recorded at frequency 500 Hz and amplitude 20 mV, to for the solution of 12 nM of ATR, in 3 mM KCl, 0.1 mM $Na_2HPO_4$, 1.8 mM $KH_2PO_4$, pH 7.0 and the redox couple $Fe(CN)_6^{3-}/Fe(CN)_6^{4-}$ 5 mM.

As shown in Fig. 7, the effect of time of AuNPs deposition on the immunosensor response for the solution containing of 12 nM of ATR, recorded at frequency 500 Hz and amplitude 20 mV, in PBS at pH=7.0.

The graph, also, shows that the value of the immunosensor, response increases with increasing the deposition time of AuNPs, which is corresponds to amount of AuNPs on the surface of the immunosensor. It can be seen that the value of the signal for the ATR solution reaches to a maximum up to 160 s, and at the higher deposition time the value of $\Delta Q$ stays constant or decrease slightly.

### 3.3. Calibration curve

As mentioned above the immunosensor response could be expressed in coulomb based on equation 8. However, the sensitivity and magnitude of the response to the addition of standard solutions of ATR depends on the choice of the integration range. For obtaining the best performance for the immunosensor the integration range of peak was selected, which was -100 to 1000 mV.
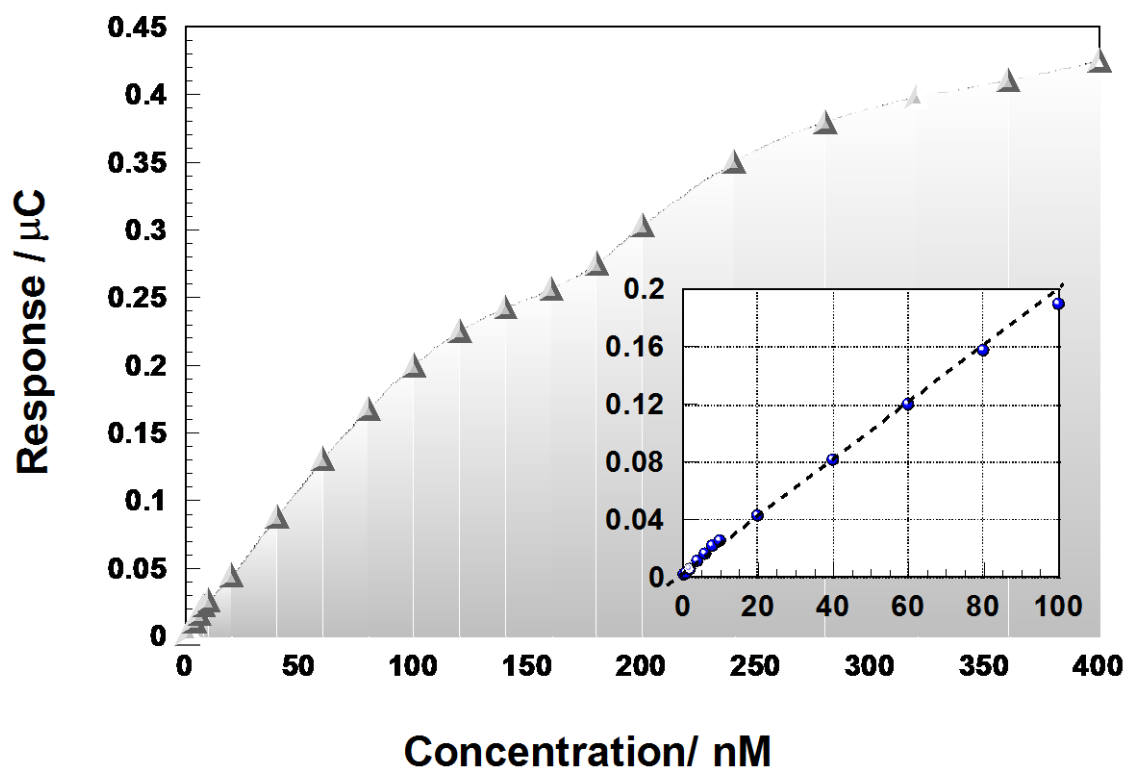


**Figure 8.** The calibration curve for ATR determination in  PBS, containing, 3 mM KCl, 0.1 mM Na$_2$HPO$_4$, 1.8 mM KH$_2$PO$_4$, pH 7.0 and the redox couple Fe(CN)$_6^{3-}$/Fe(CN)$_6^{4-}$ 5 mM, in the potential range of -100 to 1000 mV at frequency 500 Hz, and amplitude 20 mV.

Fig. 8 illustrates a typical response of the sensor based on $\Delta Q$ to set standard solutions of ATR from 0.05 to 50.0 nM in PB solution, pH 7.0. in where the experimental parameters were set at optimum values in order to obtain the best detection limits for the immunosensor. Results shown in

this figure represent the integrated signal for 3 consecutive additions of the ATR standard solutions. In this condition, the FFT-SW admittance voltammetry signal showed a linear dynamic range of 0.5 to 100 nM (Fig. 8). A correlation coefficient of $R^2=0.997$. Measurements carried out for small analyte concentrations allow the estimation of the detection limit and the linearity was evaluated by linear regression analysis. The detection limit, estimated based on signal to noise ratio (S/N=3), was found to be 0.02 nM.

In evaluation, the performances of the fabricated biosensor is compared with some of the best previously reported ATR immunosensor based on the utilization of different materials as the working electrode and different detection techniques (Table 1) and it was confirmed that the presented AuNPs in the base of the immunosensor combine with FFT-SW admittance voltammetry revealed an excellent and reproducible sensitivity for determination of ATR in sample solutions [37–43].

**Table 1.** The comparison of the proposed biosensor with the best previously reported ones based on the utilization of different materials

| Method | Electrode | Limit of detection (LOD) | Concentration range | Ref. |
|---|---|---|---|---|
| Differential pulse adsorptive stripping voltammetry (DPAdSV) | Bismuth film electrode (BiFE) | $1.4\times10^{-7}$ mol $L^{-1}$ | $6.7\times10^{-7}$ to $2.0\times10^{-5}$ mol $L^{-1}$ | 37 |
| Square wave voltammetry | Copper solid amalgam electrode | $8.16\times10^{-6}$ mol $L^{-1}$ | - | 38 |
| Adsorptive stripping voltammetric | Mercury film electrode | 0.024 µg $L^{-1}$ | 0.5 to 60 µg $L^{-1}$ | 39 |
| Continuous Flow-Square Wave Voltammetry | Hanging mercury drop electrode | 0.030 and 0.10 µg $mL^{-1}$ | 0.10 to 2.0 µg $mL^{-1}$ | 40 |
| Sequential injection-square wave voltammetry (SI-SWV) | Hanging mercury drop electrode | $2.1\times10^{-8}$ and $7.0\times10^{-8}$ mol $L^{-1}$ | $1.16\times10^{-7}$ to $2.32\times10^{-6}$ mol $L^{-1}$ | 41 |
| Anodic adsorptive stripping voltammetry | Gold microelectrode | $4.3\times10^{-7}$ mol $L^{-1}$ | - | 42 |
| Square wave voltammetry | Hanging Mercury Drop Electrode (HMDE) | 2µg$l^{-1}$ | 10 to 250 µg$l^{-1}$ | 43 |

## 4. CONCLUSIONS

In conclusion, in this paper, an ultra-sensitive immunosensor has been fabricated by modifying the GC electrode, and it is shown that the electrochemical design is crucial to the detection performance for the immunosensor described for the measurement of ATR. The ease of the one-step electrodeposition of AuNPs and the biocompatible matrix endowed the immunosensor with high reproducibility and storage stability. Both the unique FFT-SW admittance voltammetry method and the

promising performance of the developed immunosensor enable the construction of new biosensing platforms for the biological molecules. A low response time, less than 8s, and detection limit of 0.02 nM was observed. The stability of the sensor was tested, and the sensitivity retained 91.2 % of initial sensitivity up to 40 days, which gradually decreases.

## References

1. H. Martin, Pesticidal Manual: Basic Information on the Chemicals Used as Active Components of Pesticides, Ed., British Crop Protection Council, (1968), 1st ed.
2. M.E.S. Mostafa, H.M. Lotkat, and O.H.E. Hammonda, *Ecotoxicol. Environ. Saf.*, 29 (1994) 349.
3. S.Y. Kim, Y-A. Jo, J. Choi, and M.J. Choi, *Microchem. J.* 68 (2001) 163.
4. H. Katsumata, S. Kaneco, T. Suzuki, and K. Ohta, *Anal. Chem. Acta.* 577 (2006) 214.
5. G. Min, S. Wang, H. Zhu, G. Fang, and Y. Zhang, *Sci. Total Environ.* 396 (2008) 79.
6. M.K. Ross, N.M. Filipov, *Anal. Biochem.*, 351 (2006) 161.
7. G. Shen and H.K. Lee, *J. Chromatogr.*, 985 (2003) 167.
8. ARezic´, J.M. Horvat, S. Babic, and M. KasˇtelanMacan, *Sonochemistry 1*2 (2005) 477.
9. G. D'Agostino, G. Alberti, R. Biesuz, and M. Pesavento, *Biosens. Bioelectron*, 22 (2006) 145.
10. J. Amador-Hernandez, M. Velazquez-Manzanares, M.R. Guttierrez-Ortiz, B. Hernandez- Carlos, M. Peral-Torres, and P.L. Lopez-de-Alba, *J. Chil. Chem. Soc*. 50 (2005) 461.
11. S.D.W. Comber, C.D. Watts, and Y. Barbara, *Analyst*, 121 (1996) 1485.
12. E. Barsoukov, J.R. MacDonald, Impedance Spectroscopy: Theory, Experiment and Applications (second ed.), Wiley Interscience, New Jersey (2005) (Chapter 1).
13. S. Helali, C. Martelet, A. Abdelghani, M.A. Maaref, and N. Jaffrezic-Renault, *Electrochim. Acta*, 51 (2006) 5182.
14. E. Katz, I. Willner, *Electroanalysis*, 15 (2003) 913.
15. A.J. Bard, M. Stratmann, P.R. Unwin, Instrumentation and Electroanalytical Chemistry, vol. 3Wiley-VCH, New Jersey (2003) (Chapters 1–2).
16. X.L. Cui, D.L. Jiang, P. Diao, J.X. Li, R.T. Tong, and X.K. Wang, *J. Electroanal. Chem.,* 470 (1999) 9.
17. I. Navratilova, P. Skladal, *Bioelectrochemistry*, 62 (2004) 11.
18. P. Norouzi, H. Rashedi, T. Mirzaei Garakani, R. Mirshafian and M. R. Ganjali, *Int. J. Electrochem. Sci.* 5 (2010) 377.
19. P. Norouzi, M. R. Ganjali, B. Larijani, A. Mirabi-Semnakolaii, F. S. Mirnaghi, and A. Mohammadi, *Pharmazie* 63 (2008) 633.
20. P. Norouzi, M. R. Ganjali, S. Shirvani-Arani, and A. Mohammadi, *J. Pharm. Sci.* 95 (2007) 893.
21. M. R. Pourjavid, P. Norouzi, and M. R. Ganjali, *Int. J. Electrochem. Sci.* 4 (2009) 923.
22. P. Norouzi, M. R. Ganjali, M. Zare, and A. Mohammadi, *J. Pharm. Sci.* 96 (2007) 2009.
23. P. Norouzi, M. Qomi, A. Nemati, and M. R. Ganjali, *Int. J. Electrochem Sci.* 4 (2009) 1248.
24. P. Norouzi, B. Larijani, M. Ezoddin and M. R. Ganjali, *Mater. Sci. Eng. C* 28 (2008) 87.
25. M. R. Ganjali, P. Norouzi, R. Dinarvand, R. Farrokhi, and A. A. Moosavi-Movahedi, *Mater. Sci. Eng. C* 28 (2008) 1311.
26. P. Norouzi, M. R. Ganjali, and L. Hajiaghababaei, *Anal. Lett.,* 39 (2006) 1941.
27. P. Norouzi, G. R. Nabi Bidhendi, M.R. Ganjali, A. Sepehri, M. Ghorbani, *Microchim. Acta,* 152 (2005) 123.
28. P. Norouzi, M. R. Ganjali, T. Alizadeh, and P. Daneshgar, *Electroanalysis*, 18 (2006) 947.
29. M. R. Ganjali, P. Norouzi, M. Ghorbani, and A. Sepehri, *Talanta*, 66 (2005) 1225.
30. P. Norouzi, M. R. Ganjali, and P. Matloobi, *Electrochem. Commun.*, 7 (2005) 333.

31. P. Norouzi, H. Rashedi, T. Mirzaei Garakani, R. Mirshafian and M.R. Ganjali, *Int. J. Electrochem. Sci.*, 5 (2010) 377.
32. P. Norouzi, F. Faridbod, E. Nasli-Esfahani, B. Larijani, M. R. Ganjali, *Int. J. Electrochem. Sci.*, 5 (2010) 1008.
33. P. Norouzi, F. Faridbod, B. Larijani, M. R. Ganjali, *Int. J. Electrochem. Sci.*, 5 (2010) 1213.
34. P. Norouzi, M. Pirali-Hamedani, F. Faridbod, M. R. Ganjali, *Int. J. Electrochem. Sci.*, 5 (2010) 1225.
35. P. Norouzi, M. R. Ganjali, A. Sepehri, and M. Ghorbani, *Sens. Actuators B* 110 (2005) 239.
36. Q. Zhou, J. Xiao, W. Wang, G. Liu, Q. Shi and J. Wang, *Talanta* 68 (2006) 1309.
37. L.C.S. Figueiredo-Filho, D.C. Azzi, B.C. Janegitz, and O. Fatibello-Filho, *Electroanalysis* 24 (2012) 303.
38. D. De Souza, R. A. de Toledo, L. H. Mazo and S. A. S. Machado, *Electroanalysis*, 17 (2005) 2090.
39. N. Maleki, G. Absalan, A. Safavi, E. Farjami, *Anal. Chim. Acta*, 581 (2007) 37.
40. L.B.O., Dos Santos, G. Abate, J.C. Masini, *J. Brazilian Chem. Soc.* 17 (2006) 36.
41. L.B.O. Dos Santos, M.S.P. Silva, and J.C. Masini, *Anal. Chim. Acta*, 528 (2005) 21.
42. S. Morais, O. Tavares, P.C. Baptista-Paíga, and C. Delerue-Matos, *Anal. Lett.* 37 (2004) 3271.
43. L.B.O. Dos Santos, G. Abate, and J.C. Masini, *Talanta*, 62 (2004) 667.